Chapter 4
The Laguerre Collocation Method

Abstract The chapter introduces first the functional framework corresponding to the spectral collocation method based on Laguerre functions. The main advantage of these functions is the fact that they decrease smoothly to zero at infinity along with their derivatives. We speculate this behavior in imposing boundary conditions at large distances. On the half-line we solve high order eigenvalue problems, linear as well as some genuinely nonlinear third and fourth order boundary value problems. The applications come from fluid mechanics, i.e., Blasius, Falkner-Skan, density profile equation, Ekman boundary layer etc. and foundation engineering. Consequently, we avoid the empiric domain truncation coupled with various numerical technique (mainly shooting) as a strategy to solve such problems. Some second order eigenvalue problems along with singularly perturbed boundary value problems are also considered. A special attention is payed to the influence of the scaling parameter (which maps the half-line into itself) on the repartition of the Laguerre nodes. We manually tune this geometrical parameter in order resolve narrow regions with high variations of solutions, i.e., the so called boundary or interior layers. Consequently, no domain decomposition, domain truncation and shooting have been used in our numerical experiments. Based on the pseudospectra of two GEPs we comment on limitations of the linear hydrodynamic stability analysis. We also observe that the non-normality of a spectral method depends on the discretization (method itself) and at the same time on the bases of functions (polynomials) used.

Keywords Density profile equation · Ekman boundary layer · Falkner Skan problem · Laguerre collocation · Movement of a pile · Physical space differentiation

The efforts to compute solutions of two-point boundary value problems on infinite intervals are in finding ways to approximate a stable manifold, i.e., a nonincreasing solution with a limit, and part of this is done by prescribing boundary conditions which put the solution on that manifold.
U M Ascher, R M M Mattheij, R D Russel, Numerical Solution of Boundary Value Problems for Ordinary Differential Equations, 1988

C.-I. Gheorghiu, *Spectral Methods for Non-Standard Eigenvalue Problems*, SpringerBriefs in Mathematics, DOI: 10.1007/978-3-319-06230-3_4,

4.1 LC Solutions to a Third Order Linear Boundary Value Problem on the Half-Line

We introduce the method with the representative problem

$$u_{xxx} - a_1 u_{xx} - a_2 u_x + a_3 u = f,\ x \in (0, \infty),\ u(0) = u'(0) = 0,\ \lim_{x\to\infty} u(x) = 0, \tag{4.1}$$

where the coefficients $a_1(x),\ a_2(x)$ and $a_3(x),\ x \in (0, \infty)$ are smooth enough in order to guarantee a correct application of the *strong collocation technique*.

The choice of basis functions on which test and trial spaces are spannedstrongly depends on special properties of the problem at hand, as for instance the asymptotic behavior of the solution when the independent variable tends to infinity. The functional framework for collocation method is that introduced in Sect. 1.2.

Therefore we rely on interpolation operators which are built on the weighted Laguerre polynomials, i.e., on functions of the form

$$e^{-x/2} L_N(x),$$

$L_N(x)$ being the *classical Laguerre polynomial* of order N.

It is important to observe that, the interval $[0, \infty)$ can be mapped to itself by change of variables $\eta = b\widetilde{\eta}$, where b is any positive real number. This will be called the *scaling factor*. Laguerre method therefore contains a free-parameter. It means that the Laguerre interpolating process is exact for functions of the form

$$e^{-bx/2} p(x) \tag{4.2}$$

where $p(x)$ is any polynomial of degree $N - 1$ or less.

The general Laguerre interpolation process in weighted Sobolev spaces was recently systematically analyzed in the monograph [36]. However, the authors do not exploit the freedom offered by the above free parameter in LC. Instead, in our computations this parameter will play a key role.

However, the best interpolation result remains that from [3] which reads

$$\|I_N u - u\|_{\omega_0} \leq C N^{(1-m)/2} \|u\|_{H^m_{\omega_\tau}}, m \geq 1, \tag{4.3}$$

where I_N is the usual interpolation operator, the weights ω are defined as $\omega_0 := e^{-x}$, $\omega_\tau := e^{-(1-\tau)x},\ 0 < \tau < 1$ and the norms have been introduced with (1.21).

As our numerical experiments showed that the high order Laguerre differentiation matrices are to some extent polluted by round off errors for $N > 100$ (see also Fig. 4.3) this result seems to be not very encouraging. Consequently, we try to examine numerically the convergence behavior of some typical functions. Thus, we consider the following four examples of exact solutions to (4.1) with $a_1 = a_2 = a_3 = 1$.

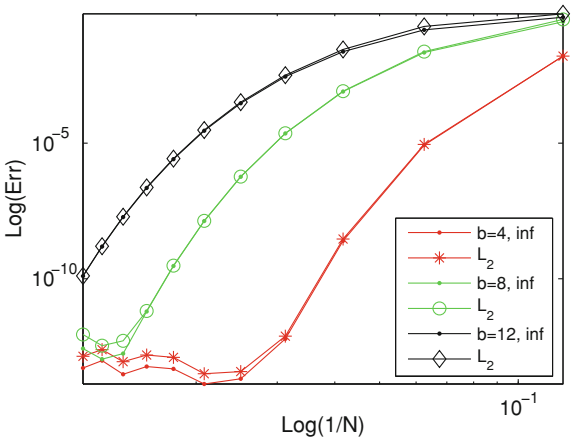

Fig. 4.1 The quasi spectral accuracy in approximating the solution (4.4) which decays at infinity without oscillations for various scaling factors b. For each and every b, one curve corresponds to inf norm and another to L_2 norm

Example 4.1 Exponential decay without oscillations at infinity

$$u(x) := x^2 e^{-x},\ x \in (0, \infty); \tag{4.4}$$

Example 4.2 Exponential decay with oscillations at infinity

$$u(x) := e^{-x} \sin^2 kx,\ x \in (0, \infty); \tag{4.5}$$

Example 4.3 Algebraic decay without oscillations at infinity

$$u(x) := \frac{x^2}{(1+x)^h}, h > 1,\ x \in (0, \infty); \tag{4.6}$$

Example 4.4 Algebraic decay with oscillations at infinity

$$u(x) := \frac{\sin^2 kx}{(1+x)^h}, h > 1,\ x \in (0, \infty), \tag{4.7}$$

for some natural k.

These functions have typical decay properties. The errors corresponding to the first case (inf and L_2 norms respectively) are reported in Fig. 4.1 when the scaling factor b as well as the cut off parameter N are simultaneously varied. It is fairly clear that the accuracy depends on both parameters. Whenever this factor is properly chosen, even for moderate values of N, the method produces results with spectral accuracy.

The presence of an oscillation factor deteriorates considerable the approximation and requires a larger interval of approximation. The situation corresponding to the second example is summarized in Fig. 4.2.

Two important conclusions can be formulated. First, as we envisage boundary layer type problems we expect an exponential decay without oscillations of solutions.

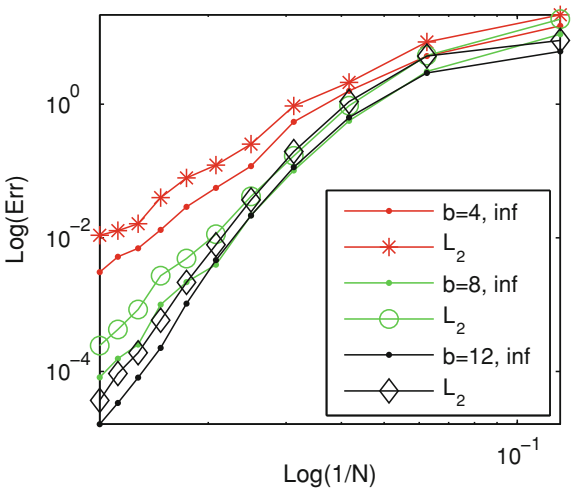

Fig. 4.2 The accuracy in approximating the solution (4.5) which decays at infinity with oscillations for various scaling factors b. For each and every b, one curve corresponds to inf norm and another to L_2 norm

Thus, the spectral accuracy could be altered only by possible nonlinearities of the problem. Second, for oscillatory decaying solutions, *mapping techniques* or even *truncation domain methods* can be a serious concurrent for Laguerre collocation. In [34], and partially in [35], the authors study the accuracy of Laguerre based Galerkin method applied to a self adjoint second order elliptic problem with similar conclusions.

4.2 The Falkner-Skan Problem

The Prandtl's boundary layer equations for flow past a flat plate in a non-uniform external flow (see for instance the well known monographs [26, 32, 33]) are reduced to the third order nonlinear differential equation

$$f''' + ff'' + \beta\left(1 - f'^2\right) = 0, \eta \in (0, \infty), \tag{4.8}$$

where β is a real parameter, the so called *Hartree parameter*, and f' stands for the velocity inside the boundary layer. This is known as the *Falkner-Skan equation*. In fact β signifies the dimensionless pressure gradient parameter and $\beta := \frac{2m}{m+1}$ where m comes from the expression of the free stream velocity $U_\infty(x) := Cx^m$, C being a real constant.

The viscous boundary conditions reduce themselves to the following three

$$f(0) = f'(0) = 0, \quad f' \to 1, \ \eta \to \infty. \tag{4.9}$$

Whenever there exists heat transfer between the wall and viscous incompressible fluid moving along, the energy equation reduces to the nonlinear second order equation

$$\vartheta'' + \Pr f \vartheta' = 0, \eta \in (0, \infty), \tag{4.10}$$

where ϑ stands for non-dimensional temperature and Pr for *Prandtl number*. Equation (4.10) is supplied with the following two boundary conditions

$$\vartheta(0) = 1, \vartheta \to 0, \quad \eta \to \infty. \tag{4.11}$$

As soon as the problem (4.8, 4.9) is solved, the problem (4.10, 4.11) becomes a linear one and is immediately solvable. The left hand side part of (4.8) is also present in the boundary layer equations of two-dimensional laminar and turbulent flows.

In order to homogenize the boundary condition at infinity in (4.9), we introduce the new unknown $F(\eta)$ by

$$F(\eta) := f(\eta) + 1 - \eta - e^{-\eta}. \tag{4.12}$$

In this new variable Eq. (4.8) and the boundary conditions (4.9) read

$$\begin{cases} F''' + \left[FF'' + e^{-\eta}\left(F + F''\right) + (\eta - 1)F''\right] \\ -\beta\left[F'^2 + 2\left(1 - e^{-\eta}\right)F'\right] = g(\eta), \quad \eta \in (0, \infty), \\ F(0) = F'(0) = 0, \ F' \to 0, \ \eta \to \infty, \end{cases} \tag{4.13}$$

where the r.h.s. term $g(\eta)$, becomes

$$g(\eta) = e^{-\eta}\left[\left(2 - \eta - e^{-\eta}\right) - \beta\left(2 - e^{-\eta}\right)\right]. \tag{4.14}$$

4.3 The Laguerre Differentiation Matrices

In order to solve the two-point boundary value problem (4.13) by LC method we represent $F(\eta)$ by the interpolate $p_{N-1}(\eta)$ defined by

$$p_{N-1}(\eta) := \sum_{j=1}^{N} \frac{e^{-\eta/2}}{e^{-\eta_j/2}} \Psi_j(\eta) F_j, \tag{4.15}$$

where $\Psi_j(\eta)$ are the Lagrangian cardinal polynomials

$$\Psi_j(\eta) := \prod_{m=1,\ m\neq j}^{N} \left(\frac{\eta - \eta_m}{\eta_j - \eta_m}\right), \ j = 1, 2, ..., N. \tag{4.16}$$

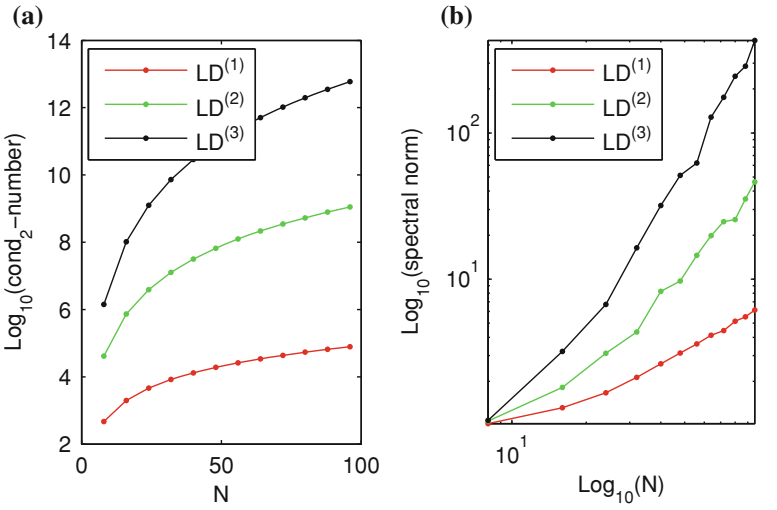

Fig. 4.3 The conditioning of the first three Laguerre differentiation matrices when the scaling factor $b = 2$; **a** the condition number versus N, and **b** the spectral radius versus N

The interpolating nodes η_j, $j = 2, ..., N$ are the roots of Laguerre polynomial of degree $N - 1$, indexed in increasing order of magnitude. We add a node $\eta_1 = 0$ in order to facilitate the incorporation of boundary conditions. Therefore we introduce the nodal unknown values $F_j = F(\eta_j)$, $j = 1, ..., N$.

In order to write down the LC equations for (4.13) we use the Laguerre differentiation matrices from the seminal paper [41] (see also [10]). Let us denote these matrices by $LD^{(n)}$, where $n = 1, 2, 3$ is the differentiation order.

Unfortunately, these matrices are fully populated, non-symmetric and quite bad conditioned. In Fig. 4.3 we report the dependence of their conditioning and of their spectral radius on N.

The Henrici number for the first, second and third order Laguerre differentiation matrices equals respectively the following numerical values: 1.1199, 1.1838 and 1.1882. These values point to a high non-normality. Our numerical experiments have revealed that this scalar measure of non-normality is practically independent of N and the scaling factor.

Thus, at least for spectral collocation method an important conclusion comes out. The non-normality depends on the method (discretization) and for a specified method it depends on the choice of bases of functions (polynomials) involved. The fourth column of Table 3.1 shows a non-normality of approximatively fourth time smaller of ChC differentiation matrices than the values displayed above. The differentiation matrices based on the functions (3.15) are into an intermediate situation.

However, a simple comparison with our results reported in Sects. 3.3 and 3.6 (see Fig. 3.13 and respectively Fig. 3.27) shows better conditioned Laguerre differentiation matrices than their Chebyshev counterpart. With respect to the spectral radius

we observe that they are of order $O(N^{0.79})$, $O(N^{1.65})$ and $O(N^{2.56})$ for the first, second and respectively third order differentiation matrices.

4.4 The LC algorithm

Boundary conditions So far, we have been mainly concerned with homogeneous Dirichlet boundary conditions which have been introduced by deleting rows and columns (see Remark 1.6). With respect to boundary value problems formulated on infinite intervals these conditions can be *behavioral*, i.e., at infinity or *numerical*, i.e., in the origin (see the influential monograph [6] for this classification). The boundary conditions at infinity are directly satisfied by Laguerre functions. In fact we have

$$d^k p_{N-1}(\eta)/d\eta^k \to 0, \ \eta \to \pm\infty, \tag{4.17}$$

for any natural number k.

Now, an arbitrary number of m homogeneous or nonhomogeneous boundary conditions at zero (or at any other fixed real point) will be introduced by a *removing technique of independent boundary conditions* initiated in [15]. With this technique, we consider the boundary conditions on the origin as some linear independent constraints on the *state* of our system of N *degrees of freedom* and remove them since they are slaved to the other $N - m$ degrees which we keep. Thus, we decompose the state of the system into degrees of freedom that we keep and degrees of freedom that we remove using a *constraint matrix*. We express the removed state variables as a function of the kept ones, thus preserving their action in the system. Moreover, we are not interested in the *evolution* of the removed degrees of freedom since we can, at any time, recover them from the kept ones using a *give back* matrix.

Remark 4.1 In most cases, we can apply the procedure described above by simple matrix manipulations, the only two rules being:

1. For Dirichlet and Neumann boundary conditions, i.e., $m = 1$, remove the mesh point where the boundary condition applies.
2. For clamped boundary conditions (Dirichlet and Neumann at the same location) or hinged, mixed boundary conditions, when $m = 2$, remove the mesh points *at* and *next to* where the boundary condition applies.

A fairly similar technique is used in [41] where the authors introduce some hinged boundary conditions in a fourth order problem.

This simple and efficient algorithm in imposing the boundary conditions in the collocation method is a serious advantage when the method is compared with the Galerkin one.

The equations of the LC method The method casts the problem (4.13) into the following nonlinear algebraic system

$$\begin{aligned}\widetilde{\widetilde{LD}}^{(3)}\widetilde{\widetilde{\mathbf{F}}}+\left[\widetilde{\widetilde{LD}}^{(2)}\left(\widetilde{\widetilde{\mathbf{F}}}.\right)^{2}+E_1\left(I+\widetilde{\widetilde{LD}}^{(2)}\right)\widetilde{\widetilde{\mathbf{F}}}+\mathbf{E}_2\widetilde{\widetilde{LD}}^{(2)}\widetilde{\widetilde{\mathbf{F}}}\right]\\ -\beta\left[\left(\widetilde{\widetilde{LD}}^{(1)}\widetilde{\widetilde{\mathbf{F}}}\right).^{2}+E_3\widetilde{\widetilde{LD}}^{(1)}\widetilde{\widetilde{\mathbf{F}}}\right]=\widetilde{\widetilde{\mathbf{g}}}.\end{aligned} \tag{4.18}$$

In (4.18) the vector $\widetilde{\widetilde{\mathbf{F}}}$ contains the nodal unknown values $F_j,\ j=3,...,N$, i.e., the kept degrees of freedom from $\mathbf{F}$. The double tilde placed over differentiation matrices $\widetilde{\widetilde{LD}}^{(i)}, i=1,2,3$ means that the first two rows and columns of the differentiation matrices $LD^{(n)}, n=1,2,3$ are deleted and the Dirichlet and Neumann boundary conditions on zero were already incorporated using the constraint matrix. The matrices $E_i,\ i=1,2,3$ are $(N-2)\times(N-2)$ diagonal matrices with the diagonal entries $e^{-\eta_k},\ \eta_k-1$ and $2\left(1-e^{-\eta_k}\right)$, respectively, and $\widetilde{\widetilde{\mathbf{g}}}$ is the vector with the components

$$g_k=e^{-\eta_k}\left[2-\eta_k-e^{-\eta_k}-\beta\left(2-e^{-\eta_k}\right)\right],\ k=3,...,N. \tag{4.19}$$

The MATLAB operators are used throughout this work and thus the elementwise power of a vector is denoted by $(\mathbf{F}.)^2$. The nonlinear algebraic system (4.18) was successfully solved by MATLAB built in function `fsolve`.

Recovering derivatives Thus, we first get $\widetilde{\widetilde{\mathbf{F}}}$ as a solution of (4.18), and then, using the give-back matrix we compute $\mathbf{F}$ and successively $\mathbf{F}'=LD^{(1)}\mathbf{F}$ and $\mathbf{F}''=LD^{(1)}\mathbf{F}'$. Equation (4.12) produces the solution of the original problem. On the precision of this recovering process we will elaborate more in the next Section.

4.5 Numerical Solutions to Falkner-Skan Problem

A non-trivial test of accuracy First, we want to test the accuracy of our algorithm for nonlinear problem (4.8, 4.9). This can be accomplished upon introducing a modified source term $\widetilde{g}(\eta)$ in the r.h.s. of (4.13) such that this problem admits the exact solution $\eta^2e^{-\eta}$. The result of integration for $f,\ f'$ and f'' was exact to a precision of order 10^{-3}. As this error persists for vanishing and non vanishing β we can assess that the nonlinearity ff'' is overwhelming responsible, comparing with $(f')^2$, for this modest accuracy. An explanation can consist in the worse conditioning of the second order differentiation matrix with respect to the first one. We have also to mention that solving the nonlinear algebraic systems throughout this Section, the procedure was convergent in each and every situation.

Falkner-Skan and some particular problems The problem (4.8, 4.9) with $\beta=0$ is the so called *Blasius problem*. Its solutions $f,\ f'$, and f'' are depicted in Fig. 4.4. The first derivative f' has the physical meaning of mean tangential velocity as a function of normal distance.

The value of the second derivative $f''(0)$, which physically means the drag on the flat plate was found to be 0.4907. This value is larger than 0.33206 frequently

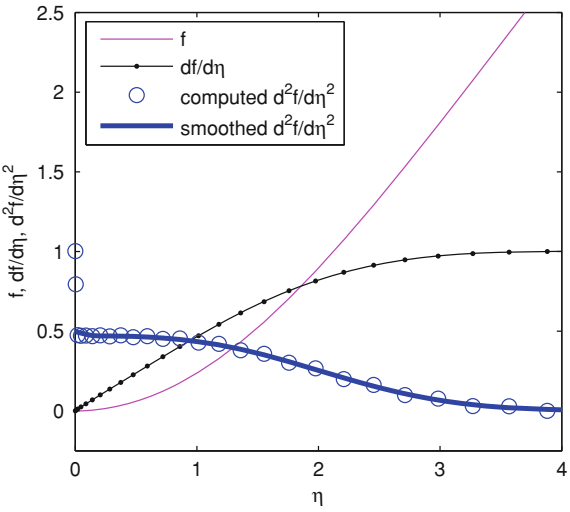

Fig. 4.4 Solution to Blasius problem when $N = 80$ and scaling factor equals 5

reported in literature and obtained by making use of shooting and domain truncation or 0.469601 reported in [30] and obtained by Fourier series. The special case $\beta = 1/2$ is called *Homann's equation*. In this case we have found $f''(0) = 0.8714...$ which is inferior to the value 0.9276... provided in [9]. The special case $\beta = 1$ is called *Hiemenz's equation* and corresponds to stagnation flow, for instance, past a large disk. In this case we have found $f''(0) = 1.1024...$ again inferior to 1.2325... furnished in the above quoted work.

With respect to our numerical results, we have to observe that very close to the flat plate the recovered values of the second derivative display a sort of numerical instability. A reason for this inconvenience can be the lack of a boundary condition for this derivative and again the round off errors which affects the second order differentiation matrix. However, with a usual cubic smoothing spline process over all recovered values of the second derivative, the first two noisy values can be removed and replaced by physically reasonable ones. This smoothing process is numerically stable with respect to N, i.e., $64 \leq N \leq 96$ and scaling factor b in the range [2,12] and is carried out with MATLAB built in function `spline`.

However, the mean velocity profile in Fig. 4.5, for positive (accelerating boundary layer flow) and negative β (decelerating boundary layer flow), shows excellent agreement with existing results in literature (see for instance [26, 32, 33]). If $\beta < 0$, so that the main stream is decreasing with respect to the longitudinal coordinate, there are two solutions of Falkner-Skan problem, provided that β is not less than -0.19884. One solution has a velocity profile of the normal 'kind', i.e., $0 \leq f'(\eta) \leq 1$, and the other has a region of reversed flow near the flat plate. A detailed discussion of the non-existence for β under this threshold is available in the monograph [1]. In our numerical experiments, for the same initial guess, i.e., equals $\mathbf{ones}(\mathbf{N-2}, \mathbf{1})$, we have obtained all normal 'kind' solutions in Fig. 4.5.

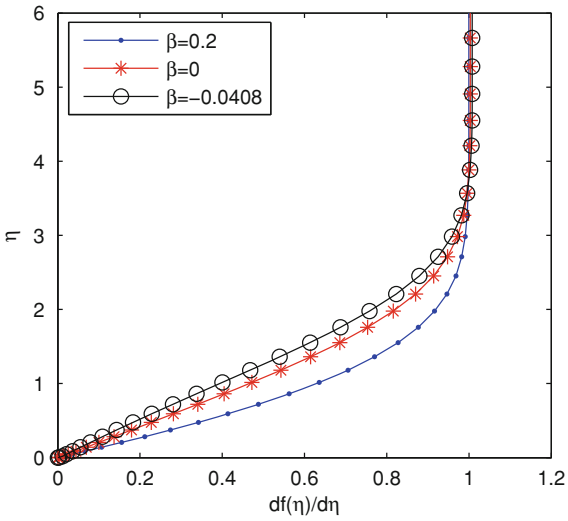

Fig. 4.5 Solutions to Falkner-Skan problem for $\beta = -0.0408,\ 0,\ 0.2$. The cut off parameter N equals 80 and scale factor equals 5

Remark 4.2 In the truncated boundary approach strategy, the boundary condition at infinity is replaced by the same condition at a given finite value L. Thus one can introduce $f_L(\eta)$ as the solution of the following problem

$$\begin{cases} f_L''' + f_L f_L'' = 0,\ 0 < \eta < L, \\ f_L(0) = f_L'(0) = 0,\ f_L'(L) = 1. \end{cases} \tag{4.20}$$

The error $e(\eta)$ related to $f_L(\eta)$ is defined by

$$e(\eta) := |f(\eta) - f_L(\eta)|,\ 0 \le \eta \le L. \tag{4.21}$$

In [31] the following upper bound for this error is provided

$$e(\eta) \le L\ f_L''(L)\ [f_L(L)]^{-1}. \tag{4.22}$$

It means that LC method used to solve this problem in our paper [11] has produced errors of order $O\left(10^{-3}\right)$ (see also Fig. 4.5). Roughly $L\ [f_L(L)]^{-1}$ approaches unity as $\eta \to L$ and thus the r. h. s. in (4.22) depends essentially on the drag at large distances away from fixed boundary.

We have to remark that in the actual computed value of $f_L(\eta)$, and its first two derivatives in L, the truncation and round off errors of the collocation are also incorporated. However, as we were not aware of the estimation (4.22) at the time the paper [11] was edited, this discussion validate once more the LC results.

4.6 Second Order Nonlinear Singular Boundary Value Problems on the Half-Line

Unsteady flow of a gas through a semi-infinite porous medium In [4, 5] the existence and uniqueness of positive solutions to some singular boundary value problems on finite and infinite intervals is established. We will consider such an example for a semi-infinite porous medium initially filled with gas at a uniform pressure. After a similarity transformation, the equation for the pressure of the gas in this medium reads

$$u''(z) = -\frac{2zu'(z)}{(1-\alpha u(z))^{1/2}},\ u(0) = 1,\ u \to 0,\ z \to \infty;\ 0 < \alpha \leq 1.$$

For $\alpha < 1$ the problem is not singular except insofar as a semi-infinite interval is involved. However, on physical grounds a solution should exists when $\alpha = 1$ (diffusion into a vacuum) even though the differential equation is singular at origin. Using LC method we have successfully solve this problem for various values of the physical parameter α. The results are displayed in Fig. 4.6. It is visible from this picture that the solutions are monotone decreasing on $[0, \infty)$ and the slope increases as $\alpha \to 1$. Thus we confirm numerically the behavior predicted theoretically in both papers quoted above.

In our recent paper [12] we have considered the following two problems.

Cohen, Fokas, Lagerstrom model The first genuinely nonlinear problem was introduced by one of the authors of [7], namely Lagerstrom (1961)

$$\begin{cases} \frac{d^2u}{dx^2} + \frac{k}{x}\frac{du}{dx} + \alpha u\frac{du}{dx} + \beta\left(\frac{du}{dx}\right)^2 = 0,\ x \in (\varepsilon, \infty), \\ u = 0\ at\ x = \varepsilon > 0, \quad u \to U, \quad x \to \infty. \end{cases} \tag{4.23}$$

The differential equation in (4.23) is the equation for the time independent temperature distribution in an infinite medium. Generally, it is somewhat an unrealistic physical model where x is a radial coordinate in $(k+1)$-dimensional space and u is the temperature. The first two terms come from Laplace operator and the last two represent nonlinear autonomous heat sources unfortunately not validated in any actual physical model. The temperature equals zero on the sphere $x = \varepsilon$, $0 < \varepsilon \ll 1$, and equals U at large distances. Using a *formal series expansion technique* Lagerstrom (1961) constructed asymptotic solutions for two ($k = 1$) and three ($k = 2$) dimensions, for $\beta = 0$ and $\beta = 1$. The intuitive reasoning indicated that for one-dimensional case ($k = 0$) the problem is not singular. This was verified by the construction of an exact solution in this case (by quadrature and inversion of a function). If $\alpha > 0$ and $\beta > 0$ one can make their values unity (even simultaneously) by a scale transformation in u and x. However, because $\beta = 0$ is an interesting case and $\alpha = 0$ occurs in an auxiliary equation, i.e., Stokes equation, we consider arbitrary nonnegative values for α and β. For $\alpha > 0$, the problem (4.23) has a unique solution.

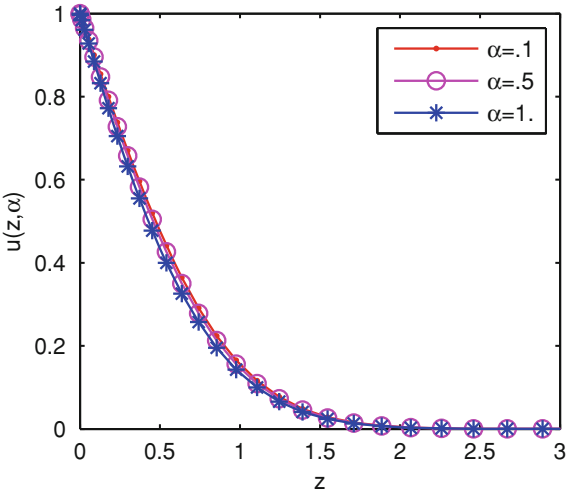

Fig. 4.6 The solution to gas flow problem when $b = 8$ and $N = 64$

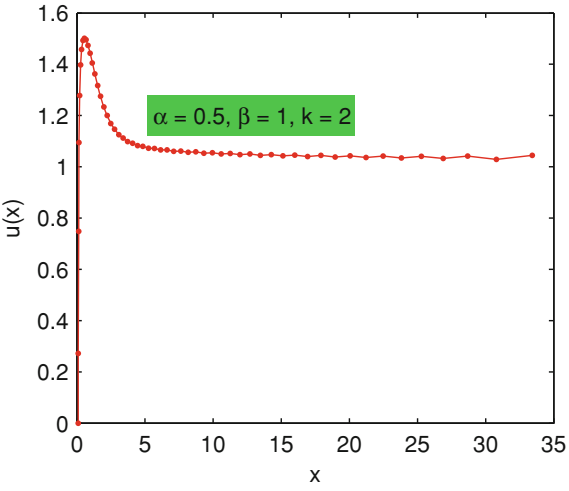

Fig. 4.7 The solution to the Cohen, Fokas and Lagerstrom problem when $b = 6$ and $N = 64$

Our LC approximation for such a solution when $\varepsilon = 0.1$ and $U = 1$ is depicted in Fig. 4.7.

Singular asymptotic techniques may and have been used only if $k \geq 1$. For $\alpha = 0$ the problem may be solved explicitly. The boundary value problem then has a solution which is unique only if $k > 1$. Thus $k = 1$ is an important limiting case.

In [16] a rigorous discussion of the existence of a solution to (4.23) for $\beta = 0,\ k = 1$, and $\varepsilon \to 0^+$ is provided. Such a solution is depicted in Fig. 4.8 for the same value of $\varepsilon,\ U,\ N,$ and b as stated above. The case $\beta = 0,\ k = 1$ has the advantage of being applicable to "real" problems, i.e., to some problems in fluid dynamics for which (4.23) could be a model.

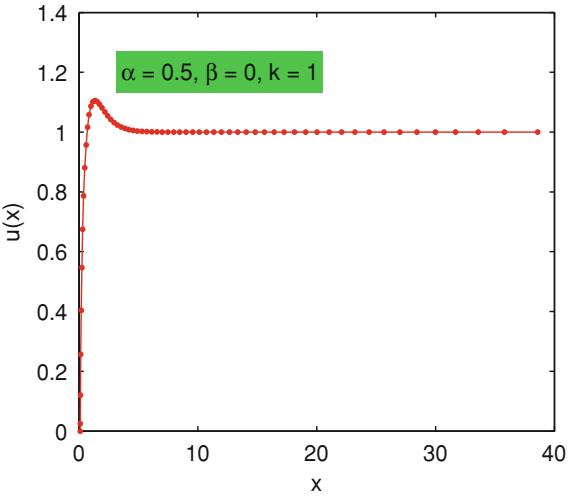

Fig. 4.8 A "real" solution to the Cohen, Fokas and Lagerstrom problem

Both curves depicted in Figs. 4.7 and 4.8 behave in perfect accordance with the asymptotic for $x \to \infty$ predicted in [24]. There is still a difference between them for large x. It seems that the nonlinearity $\beta \left(\frac{du}{dx}\right)^2$ affects to some extent the stability of the LC numerical process but ill conditioning of the differentiation matrices does not appear to be a serious problem as our experiments indicate.

Solutions to density profile equation We investigate the *monotonously increasing solutions* of the problem

$$\begin{cases} \rho''(r) + \frac{N-1}{r}\rho'(r) = 4\lambda(\rho(r)+1)\rho(r)(\rho(r)-\xi), 0 < r < \infty, \\ \rho'(0) = 0,\ \rho \to \xi,\ r \to \infty, \end{cases} \tag{4.24}$$

where $\rho(r)$ stands for the density of a fluid. For the sake of simplicity we can choose the following values of the parameters: $\lambda = 1$ without restriction of generality, $N = 3$ which corresponds to a physically meaningful case and ξ varying in the range (0,1) such as to reflect different physical situations. The above equation is called the *density profile equation* and has the origins in the Cahn-Hillard theory which is used in hydrodynamics to study the behavior of non-homogeneous fluids. In [18] the authors find by polynomial collocation the so called "bubble-type solution". Analytical aspects concerning this equation, i.e., the existence and uniqueness of strictly increasing solutions, their asymptotic behavior at infinity etc., as well as various numerical solutions were thoroughly carried out in the series of papers pagination [19, 20, 22]. When such a solution exists it has exactly one zero R in $(0, \infty)$, and R is interpreted as the bubble radius. They also satisfy $-1 < \rho(r) < \xi$ and $-1 < \rho(0) < 0$. The derivative of the solution attains a maximum at some value $\widetilde{r} < R$, and tends to 0 at infinity. Eventually, a bubble-type solution exhibits an *interior layer* which becomes sharper as $\xi \to 1$. We also have to observe that the problem

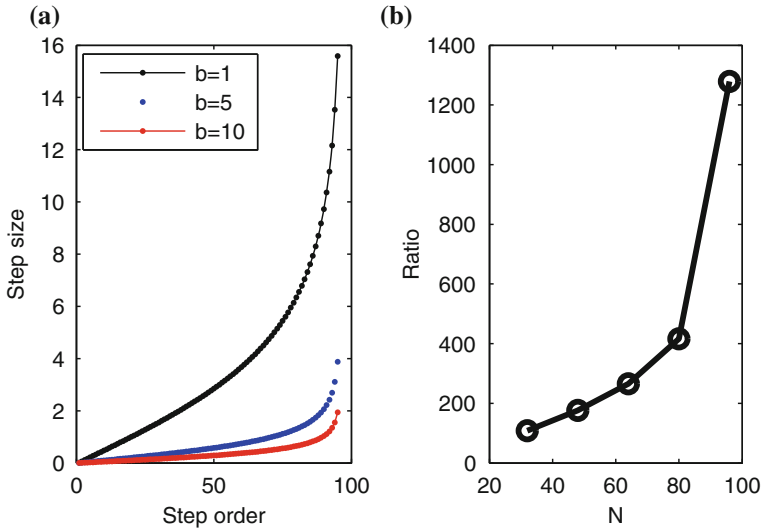

Fig. 4.9 The repartition of Laguerre nodes and step sizes for various N and b

(4.24) always admits the constant solution $\rho\,(r) = \xi$ which physically corresponds to the case of a homogeneous fluid, i.e., without bubbles.

In [18] the authors transform the problem to a finite interval and show that essential singular problem obtained is well-posed. In contrast, we solve (4.24) by LC. In fact, with respect to singularly perturbed problems, in [38], the authors observe that "for good resolution of the numerical solution at least one of the collocation points ought to lie in the boundary layer". Thus, the repartition of the Laguerre collocation nodes is of the utmost importance. We have used the repartition plotted in Fig. 4.9. For the singular problem at hand it seems fairly well suited. More precisely, for the nodes introduced with LC scheme we define by i the order of the step $[x_{i-1},\ x_i]$, $i = 3, 4, ..., N$ and by $x_i - x_{i-1}$ its step size (the length). Consequently in Fig. 4.9a we have the dependence of the step size on the step order for various values of the scaling factor. In Fig. 4.9b we represent the dependence of the ratio of the largest step size to the smallest one upon the cut off parameter of interest. We notice a high non-uniformity of used meshes which supports fine resolutions in narrow regions with rapid variations of solutions.

As a maximal value, the above defined ratio for $N = 96$ and scaling factor $b = 10$ attains $1.2790e + 03$.

The LC algorithm, after an elementary homogenization of boundary condition at infinity, casts the problem (4.24) into a nonlinear algebraic system of type (4.18).

Corresponding to $\xi = 0.17, 0.34, 0.51, 0.68$ and 0.85 the solutions to this system are displayed in Fig. 4.10. The values of unknown function ρ in 0, the radius R, the elapsed CPU time, the number of iterations and the number of function evaluations when the nonlinear algebraic systems are solved by MATLAB code `fsolve` are

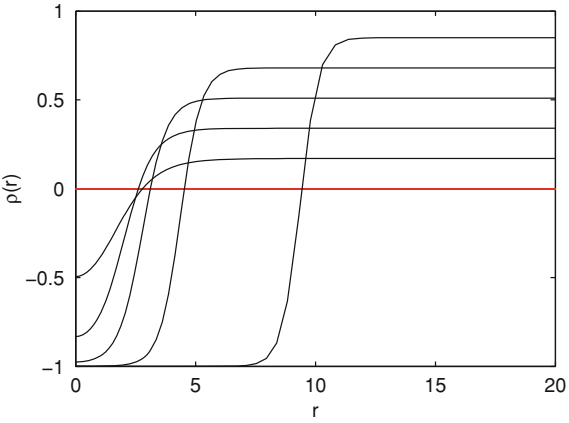

Fig. 4.10 Solutions to problem (4.24) for $\xi = 0.17, 0.34, 0.51, 0.68$ and 0.85 when $N = 64$ and $b = 10$ (from *left* to *right*)

Table 4.1 Values of solutions in 0, the bubble radius, CPU elapsed time, number of iterations and number of function evaluations when $N = 64$ and $b = 10$

ξ	$\rho(0)$	R	CPU time/s	Iter	FuncEval.
0.17	−0.49436	2.7809	0.57812	8	576
0.34	−0.83219	2.5655	0.26562	9	514
0.51	−0.97509	3.0061	0.50000	15	898
0.68	−0.99952	4.5754	3.22815	998	63.621
0.85	−0.99999	9.5451	169.016	5240	334.983

reported in Table 4.1. All computations were carried out using 2010a variant of MATLAB on an HPxw8400 workstation with clock speed of 3.2 Ghz.

We consider that the solutions displayed in Fig.4.10 reproduce correctly the similar solutions reported in [18, 22] and satisfy all analytical properties theoretically established. The computed values of $\rho(0)$ and R from Table 4.1 are fairly closed to the corresponding values displayed in the above quoted papers. It is also worth nothing that the computational effort increases as parameter ξ approaches 1. It is apparent from the last three columns of Table 4.1. The same difficulty is reported in [18]. We have paid a particular attention to the assignment of the initial guesses. Thus for the first ξ the initial guess was a straight line joining the points $(0, -1)$ and $(x_N, 1)$. Then we have used a sort of continuation, i.e., the solution just found for a ξ becomes an initial guess for the next one.

As a final word we have to remark that our numerical experiments carried out with respect to the problem (4.24) and based on mapping coupled with ChC provided totally unsatisfactory results.

Remark 4.3 Up to our knowledge a general theory for the existence (and uniqueness) of solutions to problems (4.43) is not available. Thus, in spite of the fact that we do not want to elaborate in detail on this topic, we observe that for some nonlinearity f and boundary conditions the problem could be *embedded* in the following one

$$\begin{cases} \frac{1}{p(t)}\left(p\left(t\right)u'\left(t\right)\right)' = q\left(t\right)f\left(t,u\left(t\right),u'\left(t\right)\right),\ 0 < t < \infty, \\ u(0) = 0,\ u(t)\ bounded\ on\ [0,\infty), \end{cases} \tag{4.25}$$

where $f : [0,\infty) \times \mathbb{R} \times \mathbb{R} \to \mathbb{R}$ and $p,\ \frac{1}{q} : [0,\infty) \to [0,\infty)$ are assumed to be continuous. In [27] some existence results, establishing first the solution existence on a finite interval have been proved. Then they were extended on the semi-infinite interval by Arzela-Ascoli Theorem.

4.7 Second Order Eigenvalue Problems on Half-Line

In order to get more insight into the challenging problem (4.24) we will analyze its linearization around the constant solution $\rho\left(r\right) = \xi$. It reads

$$\begin{cases} \rho''\left(r\right) + \frac{N-1}{r}\rho'\left(r\right) = 4\lambda\left(\xi + \xi^2\right)\rho\left(r\right),\ 0 < r < \infty, \\ \rho'\left(0\right) = 0,\ \rho \to \xi,\ r \to \infty. \end{cases} \tag{4.26}$$

The LC casts this problem into the following GEP

$$A\mathbf{X} = \lambda B\mathbf{X}, \tag{4.27}$$

where the matrices A and B are defined as

$$A := \widetilde{LD}^{(2)} + \mathbf{diag}\left(\frac{N-1}{\varsigma}\right)\widetilde{LD}^{(1)},\ \ b := 4\,\mathbf{diag}\left(\xi + \xi^2\right),$$

the vector ς contains the nodes $x_2,\ x_3, ..., x_N$ and the matrices $\widetilde{LD}^{(i)},\ i = 1, 2$ are defined in the manner exposed in Sect. 4.4. Therefore they incorporate the Neumann boundary condition in origin.

The pseudospectrum of this problem when $\xi = 0.4$ is provided in Fig. 4.11. Its outmost part slightly extends into the positive semi plane. On the other hand, the Henrici number, defined by (2.7), and computed for the matrix $A * B^{-1}$ is of order 1.070790. Both results suggest that the matrix pencil (A, B) is far from a normal one and consequently the linear stability analysis must be taken with some circumspection (see [39, 40]).

The eigenvalues are real and negative. The rightmost one was found to be $\lambda = -7.549523e - 004$ which implies the linear stability of constant solution.

The first five eigenvectors are available in Fig. 4.12.

All of them satisfy the boundary condition in the origin, are monotonously increasing for $0 < r < 20$ and approach with some decreasing oscillations the solution $\rho\left(r\right) = \xi$ for large r.

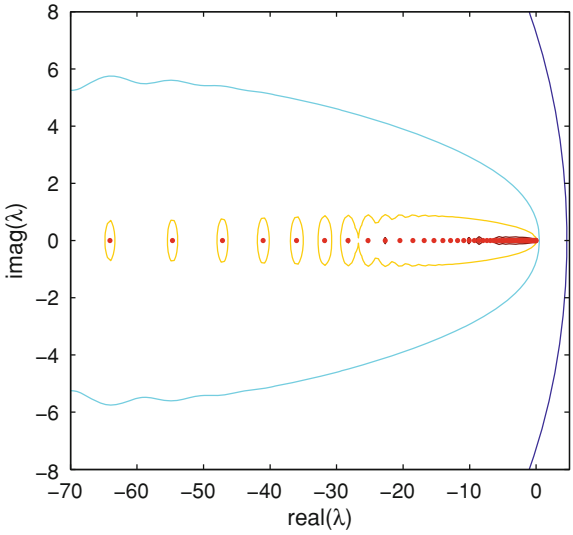

Fig. 4.11 The pseudospectrum of problem (4.26) when $b = 5$ and $N = 96$. The eigenvalues are marked with *dots*

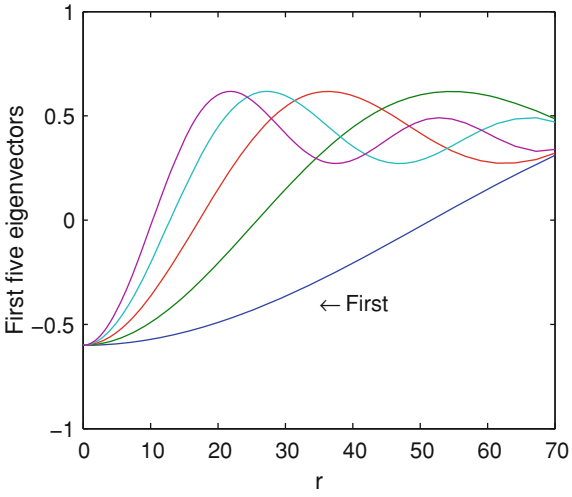

Fig. 4.12 The fist five eigenvectors (in ascending direction) of (4.26).

Throughout this work we have closely observed the eight *Rule-of-Thumb* formulated in the monograph [6]. Thus in order to test the reliability of our numerical results we repeated our numerical experiments with different N and have compared the results. Actually, in our LC scheme we have considered N in the range [64, 96].

A final remark is now opportune. Up to our knowledge there are some mathematical software packages devoted to singular S-L problems. SLEDGE is one of the most important and is described and tested in a series of papers (see for instance [28]). Beyond the computation of the eigenvalues and eigenfunctions this code attempts to classify each problem as to whether it is regular or singular, limit point or limit

circle, oscillatory or non oscillatory etc. The code is essentially based on shooting and consequently on an empirical approximation of boundary condition at infinity. On the same techniques is based the code in [29]. The LC strategy introduced above is conceptually different and tested on some non-trivial examples from these papers provided reasonable solutions.

4.8 Fourth Order Eigenvalue Problems on Half-Line

Ekman boundary layer equations In [2] the authors consider the following GEP

$$\begin{gathered}\mathbf{M}^2\phi - i\gamma R_o\left(\widetilde{U}-c\right)\mathbf{M}\phi + i\gamma R_o\widetilde{U}_{zz}\phi + 2\psi_z = 0,\\ \mathbf{M}\psi - i\gamma R_o\left(\widetilde{U}-c\right)\psi - i\gamma R_o\widetilde{V}_z\phi - 2\phi_z = 0,\end{gathered} \tag{4.28}$$

where $\mathbf{M}\phi := \phi_{zz} - \gamma^2 E_k\phi$, supplied with the boundary conditions

$$\phi(0) = \psi(0) = \phi_z(0) = 0,\ \phi,\ \phi_{zz},\ \psi \to 0,\ \ z \to \infty. \tag{4.29}$$

If E_k is set equal to unity, the Rossby number R_o equals the Reynolds number R_e and these equations are reduced exactly to those of [23]. Here γ is the wave number, $\widetilde{U}$ and $\widetilde{V}$ are two known and smooth functions and c is the complex phase speed. Equations (4.28, 4.29) define an eigenvalue problem which determines c in terms of R_o, γ and E_k.

In [14] the authors carried out a detailed analysis of this particular case, from operator theory point of view. They locate the essential spectrum and analyze the L^2 solutions of the factorized system of first order differential equations. Eventually, by domain truncation and shooting they solved numerically this system.

One important remark is now appropriate. The system (4.28, 4.29) can be transformed into a first order differential system of six equations as in [2, 14]. The converse statement is also true, i.e. eliminating for instance ϕ variable, the system can be cast into a sixth order differential equation. As the algebraic manipulations in the general case are tedious, we consider only the case when $\gamma = 0$. In this case we get the polynomial eigenvalue problem

$$\begin{gathered}-\psi^{(vi)} - 4\psi'' = 2\lambda\psi^{(iv)} + \lambda^2\psi'',\ z \in (0,\infty),\\ \psi(0) = \psi'(0) = 0,\ \psi^{(v)}(0) + 4\psi'(0) + \lambda\psi'''(0) = 0,\ \psi,\ \psi'' \to 0,\ z \to \infty,\end{gathered} \tag{4.30}$$

with boundary conditions depending on the spectral parameter. Unfortunately, from computational point of view this formulation does not open feasible perspectives.

LC solutions Rather than reproduce all the results from [2, 23] etc. we just consider one example from these papers, namely the flow profiles

$$\begin{gathered}\widetilde{U}(z) := \cos\varepsilon - \exp(-z)\cos(z+\varepsilon),\ z \in [0,\infty),\\ \widetilde{V}(z) := -\sin\varepsilon + \exp(-z)\sin(z+\varepsilon),\ z \in [0,\infty),\ |\varepsilon| < 1.\end{gathered} \tag{4.31}$$

The dependence of the leftmost eigenvalue λ on the small parameter ε, the Reynolds number R_e, and γ, is actually studied for the following LC discretization of the problem (4.28, 4.29),

$$A\mathbf{X} = \lambda B\mathbf{X}, \tag{4.32}$$

where

$$A := \begin{pmatrix} \left(-\widetilde{LD}^{(2)} + \gamma^2\right)^2 + i\gamma R_e \widetilde{V}\left(-\widetilde{LD}^{(2)} + \gamma^2\right) + i\gamma R_e \widetilde{V}'' & 2\widetilde{LD}^{(1)} \\ 2\widetilde{LD}^{(1)} + i\gamma R_e \widetilde{U}' & -\widetilde{LD}^{(2)} + \gamma^2 + i\gamma R_e \widetilde{V} \end{pmatrix}, \tag{4.33}$$

and

$$B := \begin{pmatrix} -\widetilde{LD}^{(2)} + \gamma^2 & 0 \\ 0 & I \end{pmatrix}. \tag{4.34}$$

In this GEP, $\boldsymbol{X} := \begin{pmatrix} \phi & \psi \end{pmatrix}^T$, ϕ and ψ being the unknown vectors of dimension $N-2$ and

$$\lambda := i\gamma R_e c. \tag{4.35}$$

The matrices $\widetilde{LD}^{(i)}$, $i = 1, 2$ are the differentiation matrices with the boundary conditions (4.29) introduced as in Sect. 4.4. Along with the pencil (A, B) above, we will study the pencil (A_0, B) which provides surprising information for the spectrum of GEP (4.32). The matrix A_0 reads

$$A_0 := \begin{pmatrix} \left(-\widetilde{LD}^{(2)} + \gamma^2\right)^2 & 2\widetilde{LD}^{(1)} \\ 2\widetilde{LD}^{(1)} & -\widetilde{LD}^{(2)} \end{pmatrix}, \tag{4.36}$$

and is obtained from the matrix A making $R_e = 0$.

In [25] the GEP (4.32) is solved as an optimization problem and the author finds that for the values of parameters

$$\gamma = 0.316225, \varepsilon = -23.326108^0, R_e = 54.155038, \tag{4.37}$$

the corresponding eigenvalue c has a vanishing imaginary part and the real part equals 0.616301. For the same values of the above parameters, the leftmost eigenvalue we have obtained reads

$$c = 5.563982e - 01 - i2.821821e - 02, \tag{4.38}$$

when the problem (4.32) was solved with $N = 80$ and $b = 4$. In fact, we have obtained values of the leftmost c which are indistinguishable up to the sixth digit, for

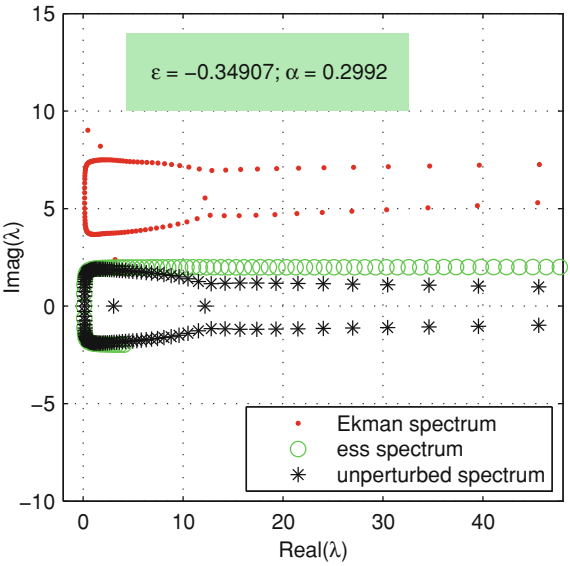

Fig. 4.13 The Ekman spectrum, essential spectrum and spectrum of the unperturbed problem

N in the range [56,96] and scaling factor in the range [2,12]. This means numerical stability of our numerical process. These numerical results are also in reasonable agreement with those published in [2, 17, 23].

In order to find the entire spectrum of the GEP we have used the `eig` MATLAB code and the accuracy of a limited number of eigenvalues from the leftmost region of this spectrum was validated using the JD algorithm (see our paper [13]).

With the aim to validate our LC results, and to compare them with the theoretical ones from [14], we have displayed the left part of the spectrum of the *unperturbed symmetric* pencil $(A_0,\ B)$ and of the spectrum of $(A,\ B)$ for values of parameters from (4.37), in Fig. 4.13.

The *essential spectrum* is indeed contained inside the predicted curve given parametrically by

$$\lambda\,(t) = t^2 + \gamma^2 + \frac{2it}{\sqrt{t^2+\gamma^2}}, \tag{4.39}$$

where t is a real parameter and i the imaginary unit. The curve is marked with circles on Fig. 4.13.

However, the spectrum of the GEP (4.32) appears to be a slightly perturbation of the symmetric spectrum of (A_0, B), i.e., the leftmost part is slightly distorted and three 'rebel' eigenvalues emerge. More than that, with Theorem 5.1 in [14], the authors show that the essential spectrum and the spectrum of the Ekman problem locate in a semi-infinite strip. Denoting $\lambda := \nu + i\mu$, this theorem predicts, in the case at hand, that $\nu \geq -1.355866e+02$ and $|\mu| \leq 4.599409e+02$. Our numerical results infer that these bounds overestimate the real situation.

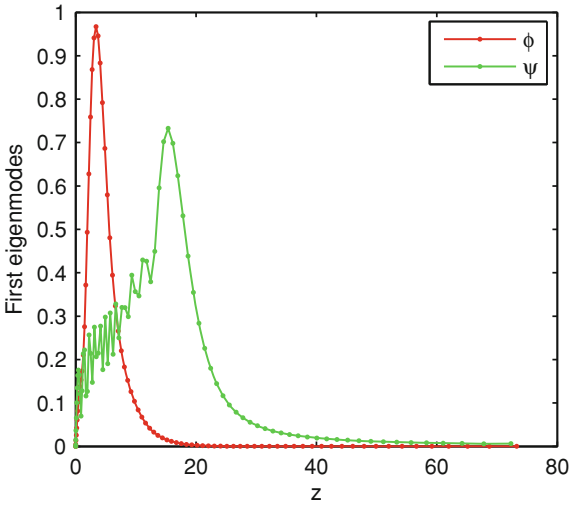

Fig. 4.14 The first eigenmodes of problem (4.32)

Moreover, the first two eigenmodes ϕ, ψ are depicted in Fig. 4.14. They behave correctly at the ends of integration interval.

We have also computed numerically the pseudospectrum of (4.32) for the values (4.37) of parameters γ, ε and R_e. It is reported in Fig. 4.15 and suggests that the pencil (A, B) in this *marginal case* is *non-normal* [see (2.9)].

Thus, according with the ideas exposed in [39, 40] this linear hydrodynamic stability analysis has to be interpreted with some precaution. In other words, the pseudospectrum of the involved algebraic GEP suggests the limitations of this analysis because it slightly extends into the left hand side semi plane.

Remark 4.4 With respect to the computational cost of the LC algorithm we have to notice the following. Once the Laguerre differentiation matrices are accurately provided by a built in function the rest of operations is carried out at a fairly low cost. The introduction of *any type of linear boundary condition* in zero is carried out by some elementary manipulations of the constraint matrix. Then a boundary value problem requires the solution of a nonlinear algebraic system and an eigenvalue one implies at least a specified region of the spectrum of a GEP. Some elementary operations with the give back matrix produce the removed degrees of freedom. The optimal value of scaling parameter has to be adjusted manually. This could be a time-consuming process which asks some computing experience and could be considered as a drawback of algorithm. However, the MATLAB built in code `fsolve` as a solver for nonlinear algebraic systems, and respectively `eig` or any of the *JD* solvers for GEPs, have worked smoothly without major incidents (non-convergent outcomes). The elapsed CPU times for all our numerical experiments have been fairly resonable.

Remark 4.5 The removing technique from Sect. 4.4 was successful in introducing the largest imaginable variety of linear boundary conditions including *slip boundary*

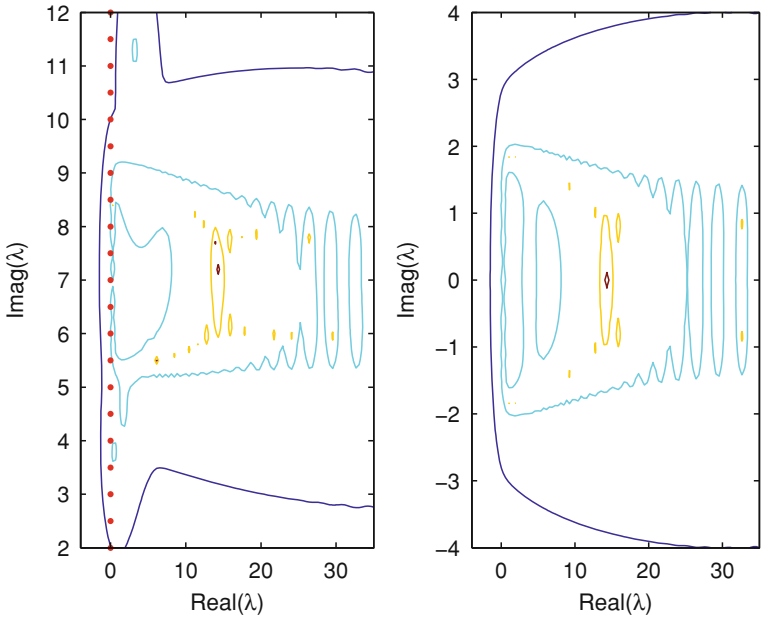

Fig. 4.15 The pseudospectrum of problem (4.32) (*left picture*) and of the unperturbed problem, when $N = 96$ and $b = 8$

conditions. Thus, we have confirmed the results of [37]. In this chapter the authors recently solved a Poiseuille flow stability problem in porous medium which involves such boundary conditions.

4.9 The Movement of a Pile

Let $u(x)$ be the deflection of a semi-infinite pile embedded in soft soil at a distance x below the surface of the soil. The governing differential equation for the movement of the pile, in dimensionless form, is given by

$$\frac{d^4u}{dx^4} = -P_1\,(1 - \exp(-P_2u)),\ 0 < x < \infty, \tag{4.40}$$

where P_1 and P_2 are positive material constants. At the origin, a zero moment and a positive shear P_3 are assumed, i.e.,

$$\frac{d^2u}{dx^2}\,(0) = 0,\ \frac{d^3u}{dx^3}\,(0) = P_3. \tag{4.41}$$

Moreover, from physical considerations it follows that $u(x)$ and all its derivatives go to zero at infinity, so that the following behavioral (asymptotic) boundary conditions

$$u,\ \frac{du}{dx} \to 0,\ x \to \infty, \tag{4.42}$$

can be imposed. The boundary value problem (4.40)–(4.42) is of interest in foundation engineering; for instance, in the design of drilling rigs above the ocean floor.

In order to solve this problem numerically we introduce the new unknown $w(x)$ by

$$u(x) := w(x) + h(x),$$

where $h(x) := x^3 e^{-x} P_3/6$. Thus, we actually solve the *homogeneous nonlinear boundary value problem*

$$\begin{cases} \frac{d^4 w}{dx^4} = -P_1 \left(1 - \exp(-P_2 \left(w + h\right))\right) - \frac{d^4 h}{dx^4},\ 0 < x < \infty, \\ \frac{d^2 w}{dx^2}(0) = 0 = \frac{d^3 w}{dx^3}(0),\ w,\ \frac{dw}{dx} \to 0,\ x \to \infty. \end{cases} \tag{4.43}$$

In [8] the author solves the problem (4.40)–(4.42) by a method based on compound matrix factorization and truncates the $[0, \infty)$ domain to a finite one. Then he compares his results with those reported in [21] where the problem is considered as a test one in working with the box difference scheme.

A theory for defining asymptotic boundary conditions to be imposed at the end of the truncated domain has been developed by many scientists but it is still unsatisfactory.

In order to avoid this serious difficulty we solve the above problem by LC method. We mention again that the important advantage of this method resides in the fact that the involved Laguerre functions automatically satisfy the boundary conditions at infinity (4.42). Details on the implementation of this method are available in our recent paper [12].

However, very sketchy, we solve numerically the non-homogeneous nonlinear algebraic system

$$\widetilde{\widetilde{LD}}^{(4)} \widetilde{\widetilde{\mathbf{w}}} = -P_1 \left(I - \exp\left(-P_2 \left(\widetilde{\widetilde{\mathbf{w}}} + \mathbf{h}\right)\right)\right) - \widetilde{\widetilde{LD}}^{(4)} \mathbf{h}, \tag{4.44}$$

where the matrix $\widetilde{\widetilde{LD}}^{(4)}$ stands for the fourth order differentiation matrix with the boundary conditions (4.41) enforced and the vectors $\widetilde{\widetilde{\mathbf{w}}}$, $\mathbf{h}$ stand respectively for the unknown vector and the vector of values of function h on the nodes x_i, $i = 3, 4, ..., N$. We mention that due to the fact that we have two independent boundary conditions in (4.41) we have to remove the first two nodes $x_1 = 0$ and x_2. Thus the system (4.44) is of order $N - 2$.

We have solved this nonlinear system starting from the initial guess, the vector **ones** of order $N - 2$. The MATLAB routine `fsolve` has used only 17 iterations and 762 function evaluations in order to get a convergent solution. Variations of this

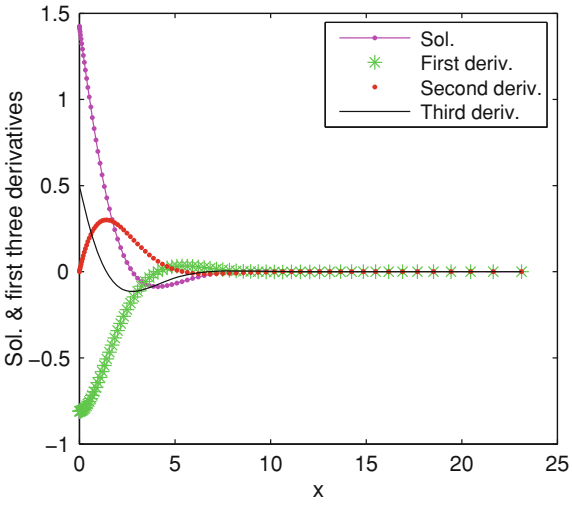

Fig. 4.16 The Laguerre collocation solution to problem (4.40)–(4.42) along with its first three derivatives when $N = 76$ and $b = 12$

initial guess, of the cut off parameter N and of the scaling factor b have led to the same solution.

Thus, we first get $\widetilde{\widetilde{\mathbf{w}}}$ as a solution of (4.44), and then, using the give-back matrix we compute the entire vector $\mathbf{w}$. Further on, by successive multiplications with first order differentiation matrix, $\mathbf{w}' = LD^{(1)}\mathbf{w}$ etc., we have recovered its derivatives of first, second and third orders (see Sect. 4.4).

The LC solution, along with its first three derivatives, to problem (4.40)–(4.42) for the values of parameters

$$P_1 = 1,\ P_2 = \frac{1}{2},\ P_3 = \frac{1}{2},$$

are depicted in Fig. 4.16. They seem to be in perfect qualitative accordance with those presented in [8].

References

1. Acheson, D.J.: Elementary Fluid Dynamics. Clarendon Press, Oxford (1992)
2. Allen, L., Bridges, T.J.: Hydrodynamic stability of the Ekman boundary layer including interaction with a compliant surface: a numerical framework. Eur. J. Mech. B Fluids **22**, 239–258 (2003)
3. Bernardi, C., Maday, Y.: Approximations Spectrales de Problems aux Limites Elliptiques. Springer, Paris (1992)
4. Baxley, J.V.: Existence and uniqueness for nonlinear boundary value problems on infinite intervals. J. Math. Anal. Appl. **147**, 122–133 (1990)
5. Bobisud, L.E.: Existence of positive solutions to some nonlinear singular boundary value problems on finite and infinite intervals. J. Math. Anal. Appl. **173**, 69–83 (1993)

6. Boyd, J.P.: Chebyshev and Fourier Spectral Methods, 2nd edn. Dover Publications, Inc., Mineola (2000)
7. Cohen, D.S., Fokas, A., Lagerstrom, P.A.: Proof of some asymptotic results for a model equation for low Reynolds number flow. SIAM J. Appl. Math. **35**, 187–207 (1978)
8. Fazio, R.: A free boundary value approach and Keller's box scheme for BVPs on infinite intervals. Int. J. Comput. Math. **80**, 1549–1560 (2003)
9. Finch, S.: Prandtl-Blasius flow. http://algo.inria.fr/csolve/bla.pdf (2008/11/12). Accessed 12 June 2012
10. Fornberg, B.: A Practical Guide to Pseudospectral Mathods. Cambridge University Press, Cambridge (1998)
11. Gheorghiu, C.I.: Laguerre collocation solutions to boundary layer type problems. Numer. Algor. **64**, 385–401 (2013)
12. Gheorghiu, C.I.: Pseudospectral solutions to some singular nonlinear BVPs. Applications in Nonlinear Mechanics. Numer. Algor. doi:10.1007/s11075-014-9834-z.
13. Gheorghiu, C.I., Rommes, J.: Application of the jacobi-davidson method to accurate analysis of singular linear hydrodynamic stability problems. Int. J. Numer. Method Fluids **71**, 358–369 (2012)
14. Greenberg, L., Marletta, M.: Numerical methods for higher order Sturm-Liouville problems. J. Comput. Appl. Math. **125**, 367–383 (2000)
15. Hoepffner, J.: Implementation of boundary conditions. http://www.lmm.jussieu.fr/hoepffner/boundarycondition.pdf (2010). Accessed 25 Aug 2012
16. Hsiao, G.C.: Singular perturbations for a nonlinear differential equation with a small parameter. SIAM J. Math. Anal. **4**, 283–301 (1973)
17. Ioss, G., Bruun, H.: True, bifurcation of the stationary Ekman flow into a stable periodic flow. Arch. Rat. Mech. Anal. **68**, 227–256 (1978)
18. Kitzhofer, G., Koch, O., Lima, P., Weinmüller, E.: Efficient numerical solution of the density profile equation in hydrodynamics. J. Sci. Comput. **32**, 411–424 (2007)
19. Konyukhova, N.B., Lima, P.M., Morgado, M.L., Soloviev, M.B.: Bubbles and droplets in nonlinear physics models: analysis and numerical simulation of singular nonlinear boundary value problems. Comput. Math. Math. Phys. **48**, 2018–2058 (2008)
20. Kulikov, G.Y., Lima, P.M., Morgado, M.L.: Analysis and numerical approximation of singular boundary value problems with p-Laplacians in fluid mechanics. J. Comput. Appl. Math. http://dx.doi.org/10.1016/j.cam.2013.09.071
21. Lentini, M., Keller, H.B.: Boundary value problems on semi-infinite intervals and their numerical solution. SIAM J. Numer. Anal. **17**, 577–604 (1980)
22. Lima, P.M., Konyukhova, N.B., Chemetov, N.V., Sukov, A.I.: Analytical- numerical investigation of bubble-type solutions of nonlinear singular problems. J. Comput. Appl. Math. **189**, 260–273 (2006)
23. Lilly, D.K.: On the instability of Ekman boundary flow. J. Atmospheric Sci. **23**, 481–494 (1966)
24. Markowich, P.A.: Analysis of boundary value problems on infinite intervals. SIAM J. Math. Anal. **14**, 11–37 (1983)
25. Melander, M.V.: An algorithmic approach to the linear stability of the Ekman layer. J. Fluid Mech. **132**, 283–293 (1983)
26. Ockendon, H., Ockendon, J.R.: Viscous Flow. Cambridge University Press, Cambridge (1995)
27. O'Regan, D.: Solvability of some singular boundary value problems on the semi-infinite interval. Can. J. Math. **48**, 143–158 (1996)
28. Pruess, S., Fulton, C.T.: Mathematical software for Sturm-Liouville problems. ACM Trans. Math. Softw. **19**, 360–376 (1993)
29. Pryce, J.D.: A test package for Sturm-Liouville solvers. ACM Trans. Math. Softw. **25**, 21–57 (1999)
30. Rosales-Vera, M., Valencia, A.: Solutions of Falkner-Skan equation with heat transfer by Fourier series. Int. Comm. Heat Mass Transf. **37**, 761–765 (2010)
31. Rubel, L.A.: An estimation of the error due to the truncated boundary in the numerical solution of the Blasius equation. Quart. Appl. Math. **13**, 203–206 (1955)

32. Schlichting, H.: Boundary Layer Theory, 4th edn. McGraw-Hill, NewYork (1960)
33. Schmid, P.J., Henningson, D.S.: Stability and Transition in Shear Flows. Springer, New York (2001)
34. Shen, J.: Stable and efficient spectral methods in unbounded domains using Laguerre functions. SIAM J. Numer. Anal. **38**, 1113–1133 (2000)
35. Shen, J., Wang, L.-L.: Some recent advances on spectral methods for unbounded domains. Commun. Comput. Phys. **5**, 195–241 (2009)
36. Shen, J., Tang, T., Wang, L.-L.: Spectral Methods. Springer, Berlin (2011)
37. Straughan, B., Harfash, A.J.: Instability in Poiseuille flow in a porous medium with slip boundary conditions. Microfluid. Nanofluid (2012). doi:10.1007/s10404-012-1131-3
38. Tang, T., Trummer, M.R.: Boundary layer resolving pseudospectral methods for singular perturbation problem. SIAM J. Sci. Comput. **17**, 430–438 (1996)
39. Trefethen, L.N.: Pseudospectra of linear operators. SIAM Rev. **39**, 383–406 (1997)
40. Trefethen, L.N., Trefethen, A.E., Reddy, S.C., Driscoll, T.A.: Hydrodynamic stability without eigenvalues. Science **261**, 578–584 (1993)
41. Weideman, J.A.C., Reddy, S.C.: A MATLAB differentiation matrix suite. ACM Trans. Math. Softw. **26**, 465–519 (2000)

http://www.springer.com/978-3-319-06229-7

Spectral Methods for Non-Standard Eigenvalue Problems
Fluid and Structural Mechanics and Beyond
Gheorghiu, C.-I.
2014, XII, 120 p. 52 illus., 49 illus. in color., Softcover
ISBN: 978-3-319-06229-7